Available online at www.sciencedirect.com
ScienceDirect
Trans. Nonferrous Met. Soc. China 26(2016) 565−574
Transactions of Nonferrous Metals Society of China
www.tnmsc.cn

Oxidative leaching behavior of metalliferous black shale in acidic solution using persulfate as oxidant

Zhi-xiong LIU[1,2], Yan-hong XIANG[1,2], Zhou-lan YIN[3], Xian-wen WU[2,4], Jian-bo JIANG[4], Yi-guang CHEN[5], Li-zhi XIONG[5]

1. College of Physics and Mechanical & Electrical Engineering, Jishou University, Jishou 416000, China;
2. The Collaborative Innovation Center of Manganese−Zinc−Vanadium Industrial Technology (the 2011 Plan of Hunan Province), Jishou University, Jishou 416000, China;
3. School of Chemistry and Chemical Engineering, Central South University, Changsha 410083, China;
4. School of Chemistry and Chemical Engineering, Jishou University, Jishou 416000, China;
5. School of Biology and Environmental Sciences, Jishou University, Jishou 416000, China

Received 12 January 2015; accepted 28 December 2015

Abstract: The oxidative dissolution of metalliferous black shale in sulfuric acid solution using sodium persulfate as an oxidant was investigated. The effects of leaching factors including leaching temperature, leaching time, stirring speed, initial concentration of sodium persulfate and sulfuric acid and particle size on the leaching rate were studied as well. The leaching kinetics of molybdenum, nickel and iron from metalliferous black shale shows that the leaching rate is controlled by a chemical reaction through a layer on the unreacted shrinking core. The leaching process follows the kinetics model $1-(1-a)^{1/3}=kt$ with apparent activation energies of 34.50, 43.14 and 71.79 kJ/mol for Mo, Ni and Fe, respectively. The reaction orders in sodium persulfate are 0.80, 1.01 and 0.75 for molybdenum, nickel and iron, respectively, while in sulfuric acid, these orders are 0.45, 0.75 and 0.50 for molybdenum, nickel and iron, respectively. In addition, the reaction mechanism for the dissolution of the metalliferous black shale was discussed.
Key words: metalliferous black shale; oxidative leaching; kinetics; sodium persulfate

1 Introduction

Nickel and molybdenum have strategic and industrial importance owning to their applications in many technological fields [1,2].

Metalliferous carbonaceous shales are organic-rich rocks that contain economically significant concentration of metals such as Mo, Ni and V [3−5], namely, these carbonaceous shales are also called Ni−Mo ores. These Ni−Mo ores are found mainly in South China, such as Zhangjiajie, Fuyang, Zunyi and Eastern Yunnan Province [5−7]. Several studies have been elaborated that the chemical composition of molybdenum can be written as the chemical formula of MoS_2 in the ores, but it is different from molybdenite. The MoS_2 in black shale exists amorphously compared with molybdenite, and the mole ratio of S to Mo is about 2.1−2.5 since there are some impurities such as MoS_3, and combination of organic carbon, clay and quartz [8]. In addition, the occurrence states of nickel in the ores are various, such as NiS_2, NiS, Ni_3S_4 and NiAsS [9,10]. Nickel and molybdenum all exist in an amorphous phase form [4,11].

In the past years, several mineral processes have been tested for treating Ni−Mo ore, such as flotation separation, gravity separation combined with flotation [12,13]. However, owing to its complex mineralogical characteristics and low metals recovery, the application of mineral dressing methods does not suit for the separation and recovery of nickel and molybdenum from Ni−Mo ore. For these reasons, researchers have to resort to the direct metallurgical processes for treating Ni−Mo ore.

Foundation item: Project (15A151) supported by the Key Research Projects of Education Department of Hunan Province, China; Project (2015JJ2115) supported by the Natural Science Fund Council of Hunan Province, China; Project (JSU071308) supported by the Construct Program of the Key Discipline in Hunan Province, China; Project (APSTIRT02) supported by the Aid Program for Science and Technology Innovative Research Team in Higher Educational Institutions of Hunan Province, China
Corresponding author: Zhi-xiong LIU; Tel: +86-743-8564492; E-mail: liuzhxi@sina.com
DOI: 10.1016/S1003-6326(16)64145-6

In recent years, many methods, such as direct alkaline leaching with hypochlorite [14] or oxygen [8,15] condition, and roasting followed by mixed alkali leaching with $NaOH/Na_2CO_3$ [16], have been used to leach molybdenum from the Ni−Mo ores. These extraction processes have been successfully used for commercial operations in China with high molybdenum extraction; however, nickel still remains in the leach residue cake, which needs to be recovered. Although the extraction of molybdenum and nickel from carbonaceous shale was investigated by oxidation roasting, sulphate roasting and water leaching [4], the high operating cost for roasting and the high capital cost for absorbent vessels of SO_2 make the cost of the metallurgical process of Ni−Mo ore prohibitively expensive.

Acid has been investigated for leaching nickel and molybdenum from Ni−Mo ore with oxidants. ZHANG et al [17] and XIAO et al [18] investigated the dissolution of nickel and molybdenum from Ni−Mo ore in acid solution with oxidants, respectively. All of these results indicate that the extraction efficiency of molybdenum is less than 70 % in HCl [17] or HNO_3 [18] solution with oxidants.

In a word, it is necessary to develop a novel metallurgical process for the dissolution of Ni−Mo ore. The process could be characterized as being environment-friendly and may be high extraction efficiency of nickel and molybdenum at low-cost.

The aim of this work is to investigate a simple leaching process for the relatively low grade No−Mo ore materials from Xiangxi region in Hunan Province, China, by using H_2SO_4 acid in the presence of $Na_2S_2O_8$ as an oxidant. This work considers the oxidative leaching kinetic about the Ni−Mo ore. The effects of the main system variables on the leaching rate were examined and the kinetic model and the apparent activation energy were determined.

2 Experimental

2.1 Materials

The Ni−Mo ore was collected from Xiangxi region in Hunan Province, China. The sample was firstly crushed to 2 mm and then ground to the required particle size of fraction ranges 75−80, 90−96, 120−125, 160−180 μm. To identify the mineral composition of the collected Ni−Mo ore, both the bulk and sieved samples were subjected to X-ray diffraction (XRD) analysis. The result of XRD is presented in Fig. 1. It indicates that there are five crystalline phases, namely, quartz (SiO_2), pyrite (FeS_2), fluorapatite ($Ca_5(PO_4)_3F$), calcite ($CaCO_3$) and epidote ($Ca_2Al_{2.6}Fe_{0.4}Si_3O_{13}H$) in the Ni−Mo ore. As seen from Fig. 1, the crystal mineral phases of molybdenum and nickel are not identified, which means that both metals may exist as amorphous phases in the Ni−Mo ore. This result agrees well with those results obtained by several researchers [4,11].

The raw ore and the different size fractions were analyzed for their major and minor elements using the reported methods [19], the results of major constituents are listed in Table 1 and the results of minor valuable elements are followed as: 0.161% Pb, 0.085% K, 0.081% Co, 0.082% Na, 0.032% Cu, 0.034%Ti, 0.028% Cr, 0.025% Se, 0.022% Mn, 0.008% Y, 0.005% Sr and 0.001% Zr. The analysis of nickel and iron was performed by an inductively coupled plasma emission spectroscopy (ICP) with a PS−6 PLASMA SPECTROVAC, BAIRD (USA), whereas molybdenum was determined with ammonium thiocyanate colorimetry by spectrophotometer [20]. The mineralogical analyses of molybdenum in the Ni−Mo ore were assayed by chemical phase analyses [21] and the results showed that that molybdenum occurred as 80.7 % MoS_2 and 19.3 % MoO_3. LIU et al [22] also claimed that molybdenum in Ni−Mo ores existed as MoS_2 and MoO_3.

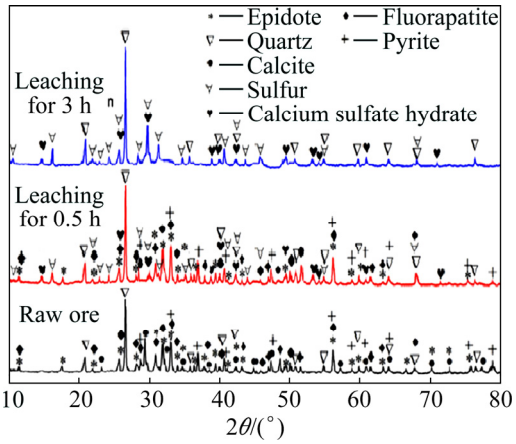

Fig. 1 XRD patterns of raw ore and residues

Table 1 Major constituents of raw ore and different factions (mass fraction, %)

Particle size	Mo	Ni	Fe	S	V	Zn	Al	Ca	As	P	Si
Raw ore	6.06	3.86	14.70	21.85	0.40	0.45	2.56	14.89	0.27	3.78	12.45
75−80 μm	6.08	3.89	14.73	21.88	0.30	0.47	2.58	14.91	0.26	3.76	12.47
90−96 μm	6.04	3.87	14.71	21.84	0.50	0.46	2.55	14.88	0.29	3.79	12.46
120−125 μm	6.07	3.84	14.74	22.79	0.40	0.43	2.57	14.92	0.25	3.81	12.48
160−180 μm	6.06	3.85	14.65	22.81	0.30	0.45	2.54	14.87	0.48	3.75	12.45

2.2 Methods

In each experiment, a flask containing 500 mL leaching solution of the desired concentrations of sulfuric acid and sodium persulfate, was submerged in a tank, the temperature was kept constant with ±0.1 K (0.1 °C). When the desired temperature was reached, 10 g Ni−Mo ore was added and the mechanical stirring started and kept at a certain stirring speed. The leaching was performed for 3 h during which 2 mL sample of the solution was taken for the determination of Mo, Ni, Fe concentrations at interval time. Molybdenum was determined with ammonium thiocyanate colorimetry by spectrophotometer. Nickel and iron, were assayed by an inductively coupled plasma emission spectroscopy (ICP). After leaching, the residue was filtered and then the leached cake was dried for 8 h at 373.15 K (100 °C). The phase of the leaching residue was characterized by a Max-Ra X-ray diffractometer.

3 Results and discussion

3.1 Effect of different oxidants on extraction of metals from Ni−Mo ore

In Ni−Mo ores, the molybdenum and nickel mainly occur as sulfides including MoS_2, NiS_2, NiS, Ni_3S_4 and NiAsS. These sulfides cannot be dissolved in acidic solution without oxidants. Therefore, the purpose of adding oxidants is to oxidize sulfides and to extract metals easily.

The experiments for leaching Ni−Mo ore with different oxidants including sodium persulfate, sodium chlorate and hydrogen peroxide were performed in the conditions of reaction time 3 h, temperature 358.15 K (85 °C), stirring speed 600 r/min, liquid-to-solid ratio 50 mL/g and initial concentration of sulfuric acid 0.5 mol/L. Initial concentration of oxidant 0.5 mol/L was used for the oxidative leaching of Ni−Mo ore. The extraction rate of metals is presented in Fig. 2. As seen from Fig. 2, the oxidation capacity order of these oxidants is $Na_2S_2O_8$>$NaClO_3$>H_2O_2. At the same time, it is observed that the extraction rate of metals using sodium persulfate as an oxidant is higher than that of metals with other oxidants. It can be explained that the standard reduction potential of persulfate (E^{Θ}=2.01 V) is higher than that of $NaClO_3$ (E^{Θ}=1.45 V) and H_2O_2 (E^{Θ}=1.77 V). However, the oxidation capacity of H_2O_2 is less than that of $NaClO_3$ in the oxidative leaching process because H_2O_2 is decomposed easily into O_2 and H_2O at 358.15 K (85 °C), and the sulfides in the Ni−Mo ore are not enough to be oxidized owing to O_2 escaping easily from the solution. Simultaneously, it may be explored that the extraction of Mo in acid solution with other oxidants reported in some literatures [17,18] is lower than that of Mo in acid solution with persulfate.

The advantage of sodium persulfate as a lixiviant in sulfuric acid solutions is that it can be made from sulfuric acid using an electrochemical cell [23]. The energy cost for making persulfate from sulfuric acid are 0.20 $/kg [24]. Once the persulfate reacts, it can return back to sulfate ions that can be converted back to persulfate. Thus, there is no consumption of the sulfuric acid used in leaching process. Therefore, sodium persulfate was determined as the oxidant for oxidative leaching of Ni−Mo ore.

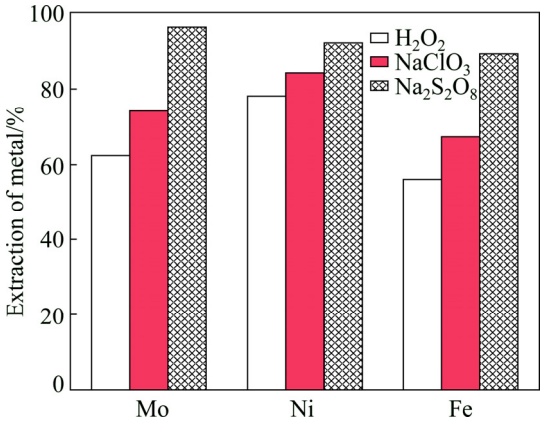

Fig. 2 Effect of different oxidants on extraction of metals in Ni−Mo ore

3.2 Phase changes and morphology during oxidation leaching

After comparison of XRD patterns in the residues with the raw Ni−Mo ore, it can be observed that calcite disappeared in the residues and all pyrite, fluorapatite and epidote disappeared in the residues after leaching for 3 h. At the same time, a new crystal phase anhydrite ($CaSO_4$) occurred in the residues. This indicates that the dissolution reactions of calcite, epidote, fluorapatite should be expressed by the following equations:

$$CaCO_3+H_2SO_4=CaSO_4+CO_2+H_2O \quad (1)$$

$$2Ca_2Al_{2.6}Fe_{0.4}Si_3O_{13}H+13H_2SO_4=4CaSO_4+0.8Fe^{3+}+6SiO_2+14H_2O+5.2Al^{3+}+9SO_4^{2-} \quad (2)$$

$$Ca_5(PO_4)_3F+5H_2SO_4=5CaSO_4+3H_3PO_4+HF \quad (3)$$

and then SiO_2 with HF may take reaction as follows:

$$SiO_2+6HF=H_2SiF_6+2H_2O \quad (4)$$

The SEM−EDS of the leaching residue whose raw was ranged from 90 to 96 μm sample is shown in Fig. 3. It indicated that the micrograph of the leaching residues indicates a progressive increase in the roughness of the solid. After 60 min leaching, the particles present some degree of degradation, which gradually increases along the progress of leaching to 180 min (Fig. 3(b)). The EDS of micro areas 1 and 2 for the residue shows that sulfur and silicon assemble onto the mineral surface. At the

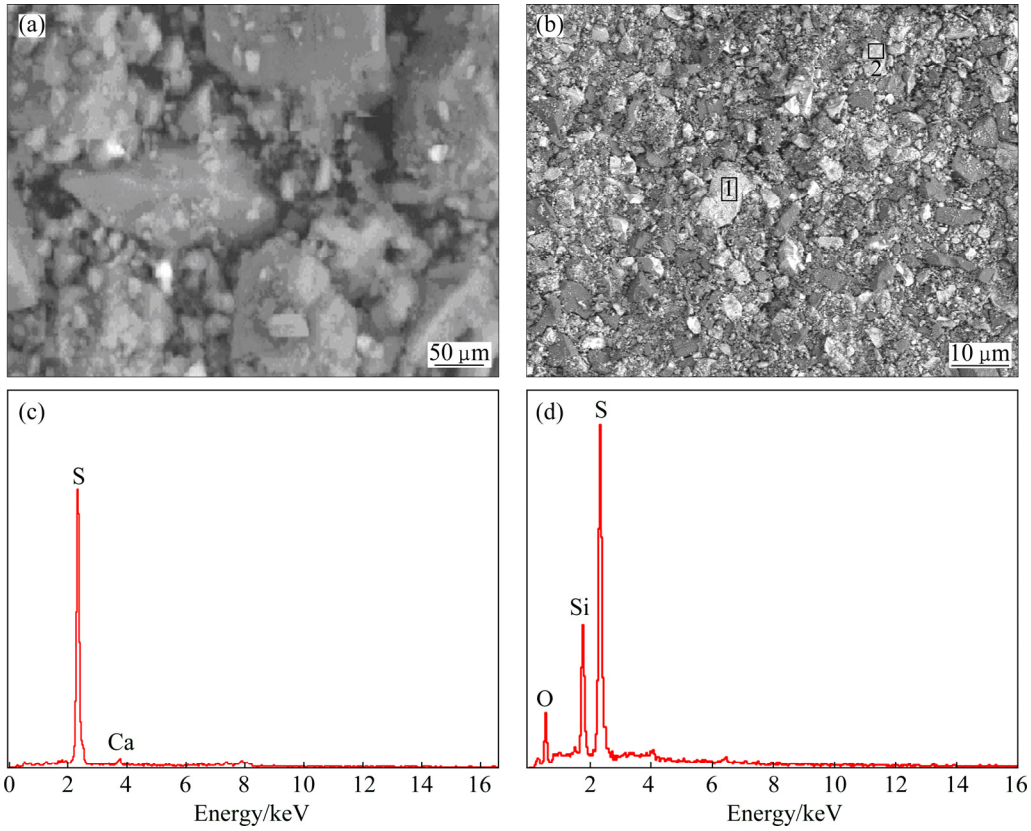

Fig. 3 SEM images of raw ore (a) and residue (b) and EDS results of areas 1 (c) and 2 (d)

same time, a new phase elemental S in the residues occurs by XRD method. The results obtained from the SEM−EDS and XRD of the residue show that the elemental sulfur is formed from the oxidation of the sulfide ores in acidic solution containing persulfate. It was reported that elemental sulfur can exist in acidic solution containing persulfate [25] and that elemental sulfur is very stable below 393 K in acid solution under an oxygen pressure and above this temperature is oxidated into SO_4^{2-} where the rate of oxidation reaction of elemental sulfur increases rapidly with temperature [26]. This indicates that the sulfides in the Ni−Mo ore may take reactions as follows:

$$MoS_2+3S_2O_8^{2-}+4H_2O=MoO_4^{2-}+8H^++6SO_4^{2-}+2S \quad (5)$$

$$NiS_2+S_2O_8^{2-}=Ni^{2+}+2SO_4^{2-}+2S \quad (6)$$

$$NiS+S_2O_8^{2-}=Ni^{2+}+2SO_4^{2-}+S \quad (7)$$

$$Ni_3S_4+3S_2O_8^{2-}=3Ni^{2+}+6SO_4^{2+}+4S \quad (8)$$

$$2NiAsS+7S_2O_8^{2-}+8H_2O= 2Ni^{2+}+14SO_4^{2-}+2AsO_4^{3-}+2S+16H^+ \quad (9)$$

$$FeS_2+S_2O_8^{2-}=Fe^{2+}+2SO_4^{2-}+2S \quad (10)$$

$$2Fe^{2+}+S_2O_8^{2-}=2Fe^{3+}+2SO_4^{2-} \quad (11)$$

3.3 Effect of stirring speed on leaching of Ni−Mo ore

The effect of the stirring speed was studied under these conditions of reaction time 3 h, temperature 358.15 K (85 °C), liquid-to-solid ratio 50 mL/g and initial concentrations of sulfuric acid 0.5 mol/L and sodium persulfate 0.5 mol/L. The ranges of stirring speeds were 150, 300, 450, 500, 550, 600 and 700 r/min. The leaching rates for molybdenum, iron and nickel increased as the stirring speed was increased to 600 r/min and remained almost constant above 600 r/min. Therefore, the optimum speed 600 r/min was used for all subsequent tests.

3.4 Effect of temperature on leaching of Ni−Mo ore

The leaching experiments were carried out with the particle size of 90−96 μm in the temperature range of 338.15−368.15 K for initial concentrations of sulfuric acid 0.5 mol/L and sodium persulfate 0.5 mol/L. The influence of temperature on the extraction of molybdenum is shown in Fig. 4. It indicates that the extraction of molybdenum increases with the temperature increasing. The change of temperature from 338.15 K to 368.15 K increases the extraction efficiency of molybdenum from 62.3 % to 98.6 %. The summarized results of the investigated metal extraction after leaching for 3 h are presented in Fig. 5. The influence of temperature on the leaching efficiency is very obvious for Mo, Ni, and Fe. An increase in temperature from 338.15 K to 368.15 K causes an increase in Ni and Fe extraction from 82.2% to 96.5% and 75.6% to 93.4%, respectively.

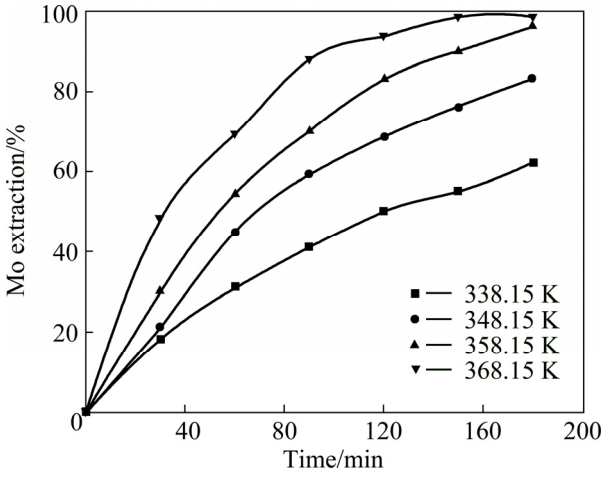

Fig. 4 Effect of temperature on molybdenum extraction

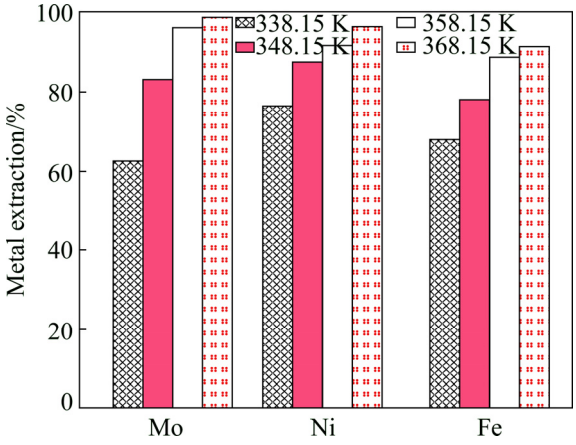

Fig. 5 Effect of temperature on Mo, Ni and Fe extraction

To control the leaching process, it is important to establish a quantitative measurement of the leaching kinetics and mechanism. The slowest step controls the whole leaching kinetics and is regarded as the rate-limiting step. The experimental data were analyzed using several models contenting the fraction reacted (a) and time (t) [27]. The two model were applied.

Spherical particles under a product layer diffusion control:

$$1-2/3a-(1-a)^{2/3}=k_d t \quad (12)$$

Spherical particles under control of chemical reaction through a layer on the unreacted shrinking core:

$$1-(1-a)^{1/3}=k_c t \quad (13)$$

where $k_d=c/d_0^2$ and $k_c=c/d_0$ are the pore diffusion rate constant and the chemical rate constant, respectively, c is constant, t is the leaching time and d_0 denotes the initial particle diameter.

Among two kinetics models tested, only Eq. (13) has been found to give a perfect straight line with a good correlation.

The plot of the data from Fig. 4 for molybdenum according to Eq. (13) versus time (t) is presented in Fig. 6(a). The values of correlation coefficients (R^2) for other examined metals are summarized in Table 2. As is seen, during the whole leaching time, the data in Fig. 6(a) and Table 2 linearly change with temperature, which indicates that the reaction rate is controlled by the chemical reaction through a layer on the unreacted shrinking core. This result obtained is different from that of the oxidative−alkaline leaching of molybdenum in the metalliferous black shale which was controlled by diffusion with the activation energy of 15 kJ/mol at higher than 338.15 K [28].

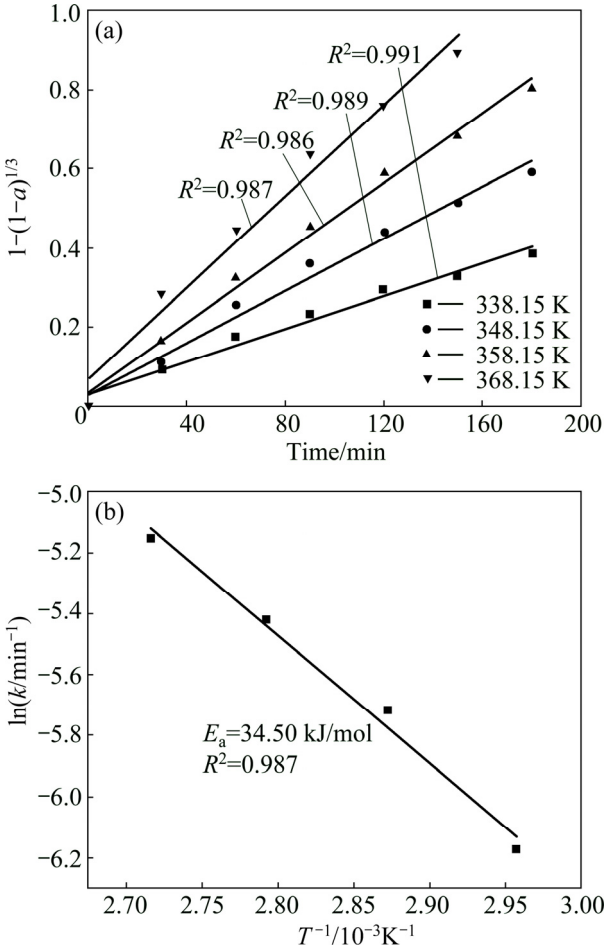

Fig. 6 Plot of date in Fig. 4 according to Eq. (13) (a) and Arrhenius plot for leaching of molybdenum (b)

Table 2 Values of correlation coefficients (R^2) of metals leaching from Ni−Mo ore in solution of 0.5 mol/L H_2SO_4 and 0.5 mol/L $Na_2S_2O_8$ depending on temperature

Temperature/K	Correlation coefficient (R^2)		
	Ni	Mo	Fe
338.15	0.991	0.991	0.993
348.15	0.998	0.989	0.996
358.15	0.995	0.996	0.995
368.15	0.993	0.987	0.992

To determine the activation energy (E_a), the plot of $\ln k$ against $1/T$ should be a straight line with a slope of $-E_a/R$ and the intercept of $\ln A$, according to the Arrhenius equation:

$$\ln k=\ln A-E_a/(RT) \quad (13)$$

where k is the apparent rate constant, A is the pre-exponential factor, R is the mole gas constant and T is the thermodynamic temperature.

The apparent rate constant k (see Table 3), obtained from the slops of the straight lines in Fig. 6(a) (for molybdenum) was used to determine the activation energy of 34.50 kJ/mol, as given on the Arrhenius plot in Fig. 6(b). Similarly, the activation energies for Ni and Fe were obtained, and the calculated values were 43.14 kJ/mol and 71.79 kJ/mol, respectively.

Table 3 Values of apparent rate constant of metals leaching from Ni−Mo ore in solution of 0.5 mol/L H_2SO_4 and 0.5 mol/L $Na_2S_2O_8$ depending on temperature

Temperature/K	$k/10^3$ min^{-1}		
	Mo	Fe	Ni
338.15	2.08	2.51	1.53
348.15	3.29	5.62	2.40
358.15	4.42	11.01	3.80
368.15	5.79	20.02	5.21

The magnitudes of activation energies found in this study support the theory that the chemical reaction is the rate-limiting step of dissolution process. Furthermore, these activation energies are close to the following calculated activation energy values: 40.40 kJ/mo1 for molybdenite in sulfuric acid solution containing hydrogen peroxide [29] and 68.8 kJ/mo1 for molybdenite in nitric acid solution under high pressure [30], 39.67 kJ/mo1 for nickel sulfide dissolution by sodium persulfate in acidic solution [25] and 83 kJ/mol for pyrite (FeS_2) leaching in acidic ferric sulfate media [31].

3.5 Effect of initial concentration of sodium persulfate on leaching of Ni−Mo ore

These experiments were performed in the presence of different initail concentrations of $Na_2S_2O_8$ varying from 0.30 to 0.60 mol/L. The other leaching conditions were fixed at temperature of 358.15 K, reaction time of 3 h, a liquid/solid ratio of 50 mL/g and an ore size of 90−96 μm. The results for molybdenum are shown in Fig. 7. The corresponding plots of $1-(1-a)^{1/3}$ versus time for molybdenum at various initial concentrations of $Na_2S_2O_8$ are graphed in Fig. 8(a). The summarized results of the metal extraction leaching for 3 h are presented in Fig. 9 at different concentrations of $Na_2S_2O_8$. An increase in initial concentration of $Na_2S_2O_8$ from 0.30 to 0.50 mol/L causes an increase in molybdenum, nickel and Fe extractions from 79.2% to 93.6%, 81.5% to 90.8% and 68.5% to 89.7%, respectively. The extractions of Mo, Ni and Fe have no significant change even when the $Na_2S_2O_8$ concentration further increases. Therefore, initial concentration of $Na_2S_2O_8$ 0.50 mol/L was chosen for the subsequent experiments.

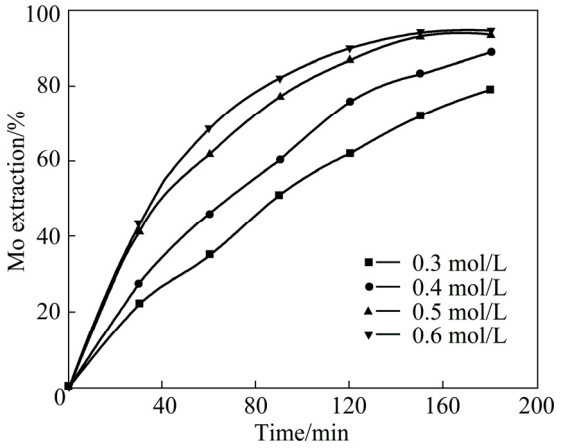

Fig. 7 Effect of initial concentration of $Na_2S_2O_8$ on molybdenum extraction

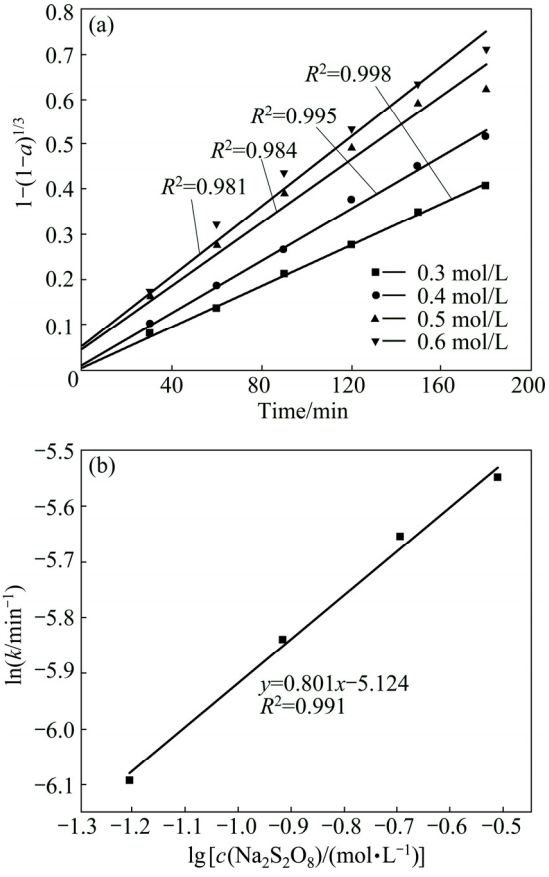

Fig. 8 Relationship between $[1-(1-a)^{1/3}]$ and leaching time for molybdenum leaching at various $Na_2S_2O_8$ concentrations (a) and plot of rate constant versus $Na_2S_2O_8$ concentration for molybdenum (b)

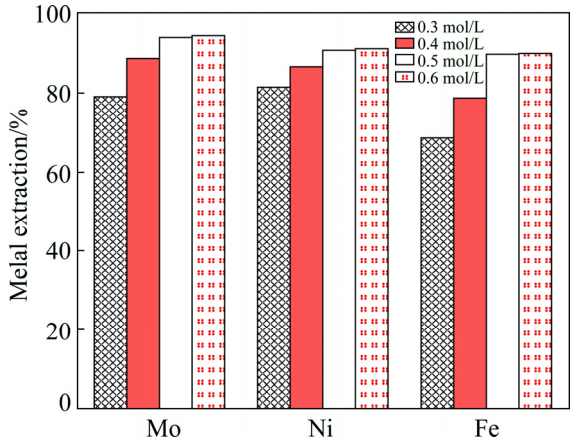

Fig. 9 Effect of $Na_2S_2O_8$ concentration on extraction of Mo, Ni and Fe

In order to obtain the reaction order of the total $Na_2S_2O_8$ concentration for molybdenum, ln$c$($Na_2S_2O_4$)−ln$k$ plot of the rate constants versus the total $Na_2S_2O_8$ concentration is plotted in Fig. 8(b). The slope of the line, or the reaction order of the total $Na_2S_2O_8$ concentration for molybdenum, is 0.801. Similarly, the reaction orders of the total $Na_2S_2O_8$ concentration for Ni and Fe according to the experimental data were calculated to be 1.01 and 0.75, respectively.

3.6 Effect of initial concentration of sulfuric acid on leaching of Ni−Mo ore

A series of leaching experiments were performed using different H_2SO_4 concentrations. The other leaching conditions were fixed as follows: initial concentration of $Na_2S_2O_8$ 0.50 mol/L, liquid-to-solid ratio of 50 mL/g, an ore size of 90−96 μm, temperature 358.15 K. The influence of H_2SO_4 concentration on the extraction of molybdenum is shown in Fig. 10. It is clear that the extraction of molybdenum increased with the initial concentration of H_2SO_4 increasing. The extraction of molybdenum increased from 93.2 % to 98.69 % when the initial concentration of H_2SO_4 increased from 0.50 to 1.10 mol/L. The summarized results of the metal extraction after leaching for 3 h are presented in Fig. 11 at different H_2SO_4 concentrations. An increase in initial concentration of H_2SO_4 from 0.50 to 1.10 mol/L causes an increase of Ni and Fe extractions from 90.7% to 97.2% and 89.6% to 94.6%, respectively.

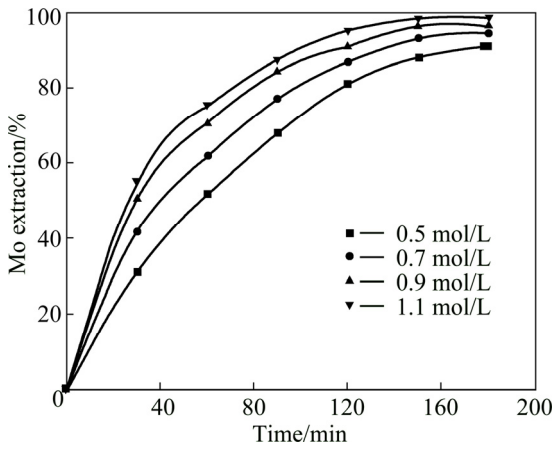

Fig. 10 Effect of H_2SO_4 concentration on molybdenum extraction

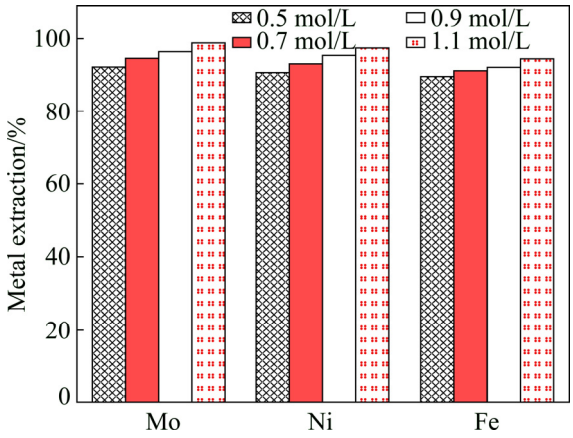

Fig. 11 Effect of initial concentration of H_2SO_4 on extraction of Mo, Ni and Fe

The corresponding plots of $1-(1-a)^{1/3}$ versus time (t) for molybdenum at various concentrations of H_2SO_4 are graphed in Fig. 12(a). In order to obtain the reaction order of the total H_2SO_4 concentration for molybdenum, ln c(H_2SO_4)–ln k plots of the rate constants versus the total H_2SO_4 concentration are plotted in Fig. 12(b). The slope of the line, or the reaction order of the total H_2SO_4 concentration for molybdenum, is 0.45. Similarly, the reaction orders of the total H_2SO_4 concentration for Ni and Fe according to the experimental data were calculated to be 0.70 and 0.50, respectively.

3.7 Effect of particle size on leaching of Ni−Mo ore

The influence of particle diameter on the extraction of metals was examined by measuring the reaction rate for fractions of four sizes: 75−80, 90−96, 120−150, 160−180 μm in a solution containing 0.5 mol/L H_2SO_4 and 0.5 mol/L $Na_2S_2O_8$ at 358.15 K with a leaching time of 150 min. The results for nickel are given in Fig. 13. As expected, the smaller the particle sizes, the faster the extraction of metals. After being ground, the spherical shape of the grains of the Ni−Mo ore was obtained. As a result, description of the kinetic curves for chemical reaction control model based on the spherical grains was found to be suitable for this purpose ($1-(1-a)^{1/3}=kt$).

The data from Fig. 14 for nickel were analyzed according to Eq. (13). The data presented in Fig. 14(a) and the calculated apparent rate constants are plotted

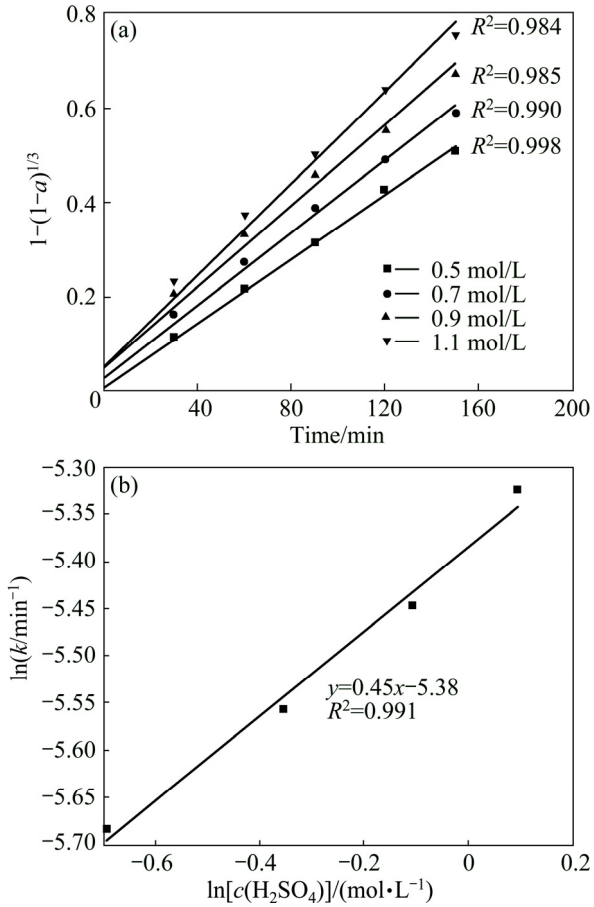

Fig. 12 Relationship between $[1-(1-a)^{1/3}]$ and leaching time for molybdenum leaching at various H_2SO_4 concentrations (a) and plot of rate constant versus H_2SO_4 concentration (b)

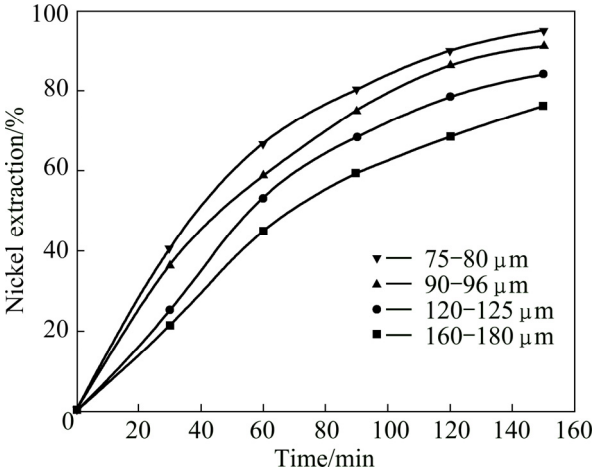

Fig. 13 Effect of particle size on nickel extraction

versus the inverse of the initial particle diameter d_0 (Fig. 14(b)). The linear relationship between the rate constant k and the inverse of d_0 indicates that the chemical reaction through a layer on the unreacted shrinking core is indeed the rate-limiting step of the dissolution process.

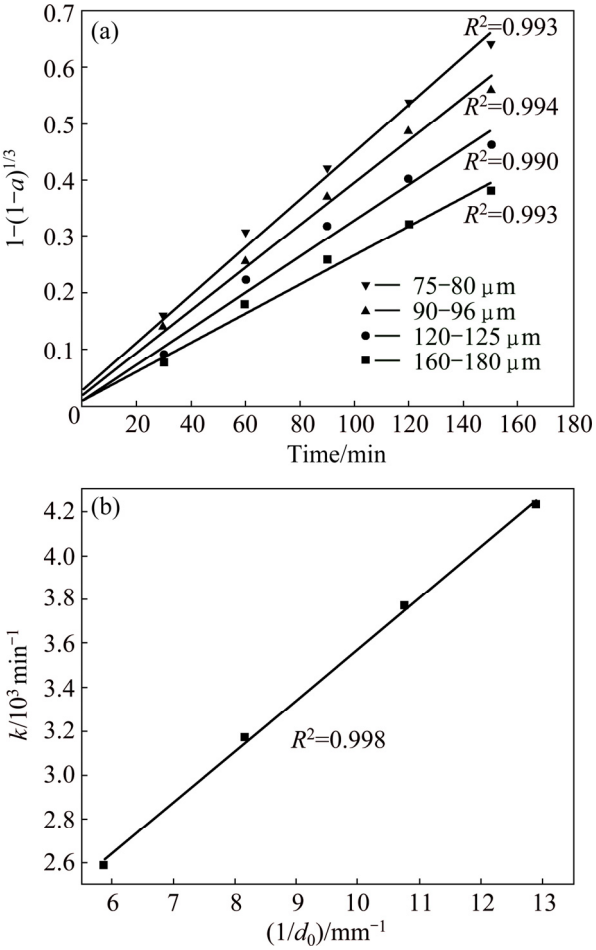

Fig. 14 Plot of variation of $1-(1-a)^{1/3}$ with time for various particle diameters (a) and rate constant versus initial particle diameter d_0 of Ni−Mo ore (b)

4 Conclusions

1) The dissolution kinetics of Ni−Mo ore was investigated in acid solution with sodium persulfate. The effects of leaching factors including leaching time, temperature, stirring speed, particle size, initial concentration of sulfuric acid and initial concentration of these oxidants such as $Na_2S_2O_8$, $NaClO_3$ and H_2O_2 were studied as well.

2) The oxidation capacity order of these oxidants is $Na_2S_2O_8$>$NaClO_3$>H_2O_2 on the leaching of Ni−Mo ore and sodium persulfate is chosen to be the oxidant for leaching Ni−Mo ore. The influence of temperature on the leaching Ni−Mo ore is very obvious in the cases of Mo, Ni and Fe.

3) The leaching process follows the kinetics model $1-(1-a)^{1/3}=kt$. The values of the apparent activation energies of 34.50, 43.14 and 71.79 kJ/mol for Mo, Ni and Fe, respectively, support the conclusion that the dissolution rate is controlled by the chemical reaction through a layer on the unreacted shrinking core.

4) The reaction orders in sodium persulfate are 0.80, 1.01 and 0.75 for Mo, Ni and Fe, respectively, while in the sulfuric acid these orders are 0.45, 0.75 and 0.50 for Mo, Ni and Fe, respectively.

References

[1] GRAWAL A, BAGCHI D, KUMARI S, KUMAR V, PANDEY B D. Recovery of nickel powder from copper bleed electrolyte of an Indian copper smelter by electrolysis [J]. Powder Technology, 2007, 177(3): 133−139.

[2] ARCHANA S, KHURANA U, YADAV S K, TANDON S N. Investigated on the extraction of molybdenum and rhenium values from low grade molybdenite [J]. Hydrometallurgy, 1996, 41(1): 99−105.

[3] KŘÍBEK B, SÝKOROVÁ I, PAŠAVA J, MACHOVIČ V. Organic geochemistry and petrology of barren and Mo−Ni−PGE mineralized marine black shales of the lower cambrian niutitang formation (South China) [J]. International Journal of Coal Geology, 2007, 72(3−4): 240−256.

[4] WANG Ming-yu, WANG Xue-wen. Extraction of molybdenum and nickel from carbonaceous shale by oxidation roasting, sulphation roasting and water leaching [J]. Hydrometallurgy, 2010, 102(1−4): 50−54.

[5] CAO Jian, HU Kai, ZHOU Jie, SHI Chun-hua, BIAN Li-zeng, YAO Su-ping. Organic clots and their differential accumulation of Ni and Mo within early Cambrian black-shale-hosted polymetallic Ni−Mo deposits, Zunyi, South China [J]. Journal of Asian Earth Sciences, 2013, 62(1): 531−536.

[6] RAYMOND M C Jr, NANSHENG C. Ni−Mo−PGE−Au-rich ores in Chinese black shales and speculations on possible analogues in the United States [J]. Mineralium Deposita, 1991, 26 (2): 83−88.

[7] JAMES B M, RAYMOND M C Jr, RICHARD I G., STEWART C E, KEVIN L S. Cyclic variations of sulfur isotopes in Cambrian stratabound Ni−Mo−(PGE−Au) ores of southern China [J]. Geochimica et Cosmochimica Acta, 1994, 58(7): 1813−1823.

[8] ZHAO Zhong-wei, LI Jiang-tao, CAO Cai-fang, HUO Guang-sheng, ZHANG Gang, LI Hong-gui. Recovery and purification of molybdenum from Ni−Mo ore by direct air oxidation in alkaline solution [J]. Hydrometallurgy, 2010, 103(1−4): 68−73.

[9] ORBERGER B, VYMAZALOVA A, WAGNER C, FIALIN M, GALLLIEN J P, WIRTH R, PASAVA J, MONTAGNAC G. Biogenic origin of intergrown Mo-sulphide- and carbonaceous matter in lower Cambrian black shales (Zunyi Formation, southern China) [J]. Chemical Geology, 2007, 238(3−4): 213−231.

[10] PAN Jia-yong, MA Dong-sheng, XIA Fei, CHEN Shao-hua, CAO Shuang-lin, GUO Guo-lin, XIE Gui-zhen. Study on nickel and molybdenum minerals in Ni−Mo sulfide layer of the lower cambrian black rock series [J]. Acta Mineralogical Sinica, 2005, 25(3): 283−288. (in Chinese)

[11] CHEN Jia-wu, GAO Cong-jie, ZHANG Qi-xiu, XIAO Lian-sheng, ZHANG Gui-qing. Leaching of nickel-molybdenum sulfide ore in membrane biological reactor [J]. Transactions of Nonferrous Metals Society of China, 2011, 21(6): 1395−1401.

[12] CHEN Dai-xiong, TANG Mei-lian, XUE Wei, XU Yan, XIE Chao. Study on dressing concentrate of high carbon nickel-molybdenum ore [J]. Hunan Nonferrous Metallurgy, 2006, 22(6): 9−11. (in Chinese)

[13] LIU Jian-dong, SUN Wei, SU Jian-fang, SUN Lei, ZHANG Gang, HU Yue-hua. Flotation performance of new type collector black shale ore [J]. Metal Mine, 2010, 403(1): 90−93. (in Chinese)

[14] WU Hai-guo. Ni−Mo carbon molybdenum smelting of nickel ore to test new technology research [J]. Hunan Nonferrous Metallurgy, 2008, 24(2): 16−18. (in Chinese)

[15] PENG Jian-rong, YANG Da-jin, CHEN Jia-xi, YAN Jiang-feng. Experimental study on alkaline leaching of crude molybdenite under pressure of oxygen [J]. Chinese Journal of Rare Metals, 2007, 31(6): 111−113. (in Chinese)

[16] WANG Ming-yu, WANG Xue-wen, LIU Wan-li. A novel technology of molybdenum extraction from low grade Ni−Mo ore [J]. Hydrometallurgy, 2009, 97(1−2): 126−130.

[17] ZHANG Bang-sheng, JIANG Kao-xi, WANG Hai-bei. Study on new technology of acid pressure leaching on Ni−Mo ore [J]. Non-ferrous Metal: Section of Smelting, 2012, 11(1): 10−12. (in Chinese)

[18] XIAO Chao-long, XIAO Lian-sheng, GONG Bo-fan, GUO Chao. Study on hydrometallurgical leaching of Ni−Mo ore [J]. Rare Metals and Cemented Carbides, 2010, 38(4): 1−6. (in Chinese)

[19] Institute of Chemistry Inspection of Beijing General Research Institute of Mining and Metallurgy. Analytical handbook of nonferrous metallurgy [M]. Beijing: Metallurgical Industry Press, 2004: 202−203. (in Chinese)

[20] MARCZENKO Z. Spectrophotometric determination of elements [M]. New York: John Wiley and Sons, 1986: 107−406.

[21] LIU Yong-qin. Chemical phase analysis of ore and industrial products [M]. Beijing: Metallurgical Industry Press, 1992: 210−214. (in Chinese)

[22] LIU Wei-ping, XU Hui, YANG Xi-yun, SHI Xi-chang. Extraction of molybdenum from low-grade Ni−Mo ore in sodium hypochlorite solution under mechanical activation [J]. Minerals Engineering, 2011, 24(14): 1580−1585.

[23] CAÑIZARES P, LARRONDO F, LOBATO J, RODRIGO M A, SÁEZ C. Electrochemical synthesis of peroxodiphosphate using boron-doped diamond anodes [J]. Journal of Electrochemical Society, 2005, 52(11): 191−196.

[24] KIMIZUKA K, KAJIWARA S, KOGURE N, TSURUGA T. Process for producing sodium persulfate: US Patent Application Publication, US2001/00115322A1 [P]. 2001.

[25] XUE Juan-qin, LU Xi, DU Ye-wei, MAO Wei-bo, WANG Yu-jie, LI Jing-xian. Ultrasonic-assisted oxidation leaching of nickel sulfide concentrate [J]. Chinese Journal of Chemical Engineering, 2010, 18(6): 948−953.

[26] JEAN P C, KIKINDAI T. The aqueous oxidation of elemental sulfur and different chemical properties of the allotropic forms S_λ and S_μ [J]. Journal of Inorganic and Nuclear Chemistry, 1981, 43(1): 9−15.

[27] LEVENSPIEL O. Chemical reaction engineering [M]. New York: Wiley, 1972: 361−371.

[28] ZHAO Zhong-wei, ZHANG Gang, HUO Guang-sheng, LI Hong-gui. Kinetics of atmospheric leaching molybdenum from metalliferous black shales by air oxidation in alkali solution [J]. Hydrometallurgy, 2009, 97(3−4): 233−236.

[29] LASHEEN T A, EL-AHMADY M E, HASSIB H B, HELAL A S. Oxidative leaching kinetics of molybdenum-uranium ore in H_2SO_4 using H_2O_2 as an oxidizing agent [J]. Frontiers of Chemical Science and Engineering March, 2013, 7(1): 95−102.

[30] KHOSHNEVISAN A, YOOZBASHIZADEH H, MOZAMMEL M, SADRNEZHAAD S K. Kinetics of pressure oxidative leaching of molybdenite concentrate by nitric acid [J]. Hydrometallurgy, 2012, 111: 52−57.

[31] BOUFFARD S C, RIVERA-VASQUEZ B F, DIXON D G. Leaching kinetics and stoichiometry of pyrite oxidation from a pyrite–marcasite concentrate in acid ferric sulfate media [J]. Hydrometallurgy, 2006, 84(3−4): 225−238.

金属黑色页岩在过硫酸盐酸性溶液的氧化浸出行为

刘志雄[1,2]，向延鸿[1,2]，尹周澜[3]，吴贤文[2,4]，蒋剑波[4]，陈义光[5]，熊利芝[5]

1. 吉首大学 物理与机电工程学院，吉首 416000；
2. 吉首大学 湖南省 211 计划锰锌钒工业技术协同创新中心，吉首 416000；
3. 中南大学 化学化工学院，长沙 410083；
4. 吉首大学 化学化工学院，吉首 416000；
5. 吉首大学 生物资源与环境科学学院，吉首 416000

摘　要：研究金属黑色页岩在过硫酸钠酸性溶液中的氧化浸出行为。考察了反应温度、浸出时间、搅拌速度、过硫酸钠和硫酸的浓度、矿物颗料的尺寸等因素对氧化浸出速度的影响。结果表明：黑色页岩中钼、镍和铁的浸出行为受化学反应速度控制，浸出过程的动力学模型为 $1-(1-a)^{1/3}=kt$，且钼、镍及铁的表观活化能分别为 34.50, 43.14 和 71.79 kJ/mol；对于过硫酸钠，钼、镍和铁的反应级数分别为 0.80, 1.01 和 0.75；对于硫酸，钼、镍和铁反应级数分别为 0.45, 0.75 和 0.50。此外，对金属黑色页岩的溶解反应机理进行了探讨。

关键词：金属黑色页岩；氧化浸出；动力学；过硫酸钠

(Edited by Yun-bin HE)